

A Decentralized Approach To Elementary Formation Maneuvers

Jonathan R. T. Lawton Brett J. Young Randal W. Beard

Keywords

Robot Formation Control, Coordinated Control, Passivity-Based-Control.

J.R.T. Lawton and B. J. Young are a graduate research assistants and R. W. Beard is an assistant professor in the Electrical and Computer Engineering Department at Brigham Young University, Provo, Utah 84602. Email: lawtonj@ee.byu.edu, young@ee.byu.edu, beard@ee.byu.edu. R.W. Beard is the corresponding author.

Abstract

This paper presents the coupled dynamics approach to executing Elementary Formation Maneuvers (EFM) for Hilare-type mobile robots. The concept of an EFM is presented. It is then shown that each of these EFMs posses a common mathematical structure and thus may be executed by the same type of robot control. We present three different EFM controls in this paper. The first puts feedback on the relative motion and the global motion of each robot. The second control adds inter-robot damping. And the third control uses saturated inputs on the relative motion and the global motion of each robot. We present simulation and hardware results for each of these controls.

I. INTRODUCTION

Cooperative robots can often be used to perform tasks that are too difficult for a single robot to perform alone. For example a group of robots can be used for moving large awkward objects [1], [2] or for moving a large number of objects [3]. In addition groups of robots can be used for terrain model acquisition [3], planetary exploration [4] or measuring radiation levels over a large area [5]. In [6] a group of robots are used for path obstruction. This could be used to impede the motion of an intruder.

Many of these tasks can be performed by controlling the robots to move in formation. For example, the radiation, exploration and terrain model acquisition problems involve making many measurements over a large area. Formation maneuvers can be used to systematically observe a large area. This can be accomplished via the following steps

1. Initialize the formation into a circle as in Figure 1a.
2. Take necessary measurements from this initial orientation.
3. Rotate the formation as in Figure 1b and repeat the observations.
4. Iteratively repeat step 3 until the entire circumference of the circle has been observed.
5. Iteratively expand or contract the formation as shown in Figure 1c
6. Once a given area has been sufficiently observed translate the entire formation as shown in Figure 1d in order to observe a different region.

Additionally when moving a large or awkward object, the group of robots must move in close formation, in order to avoid dropping the object. A formation translation could be used to move the object from some initial location to a desired final location (see Figure 1d).

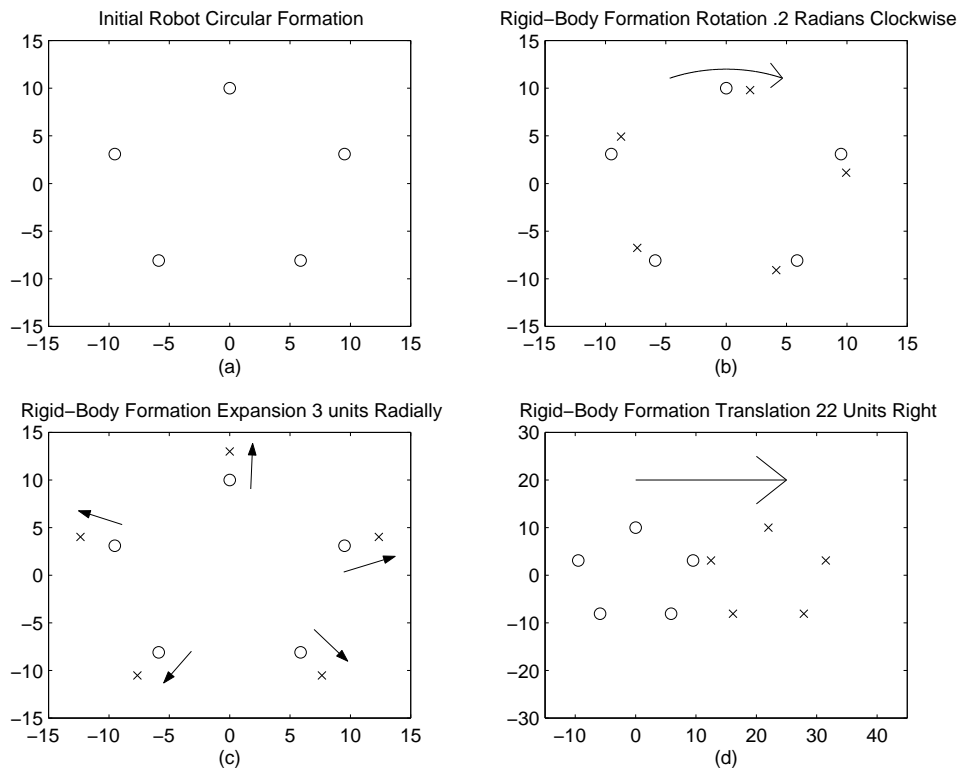


Fig. 1. Elementary Formation Maneuvers: "o" represents robot positions before and "x" represents desired robot positions after the maneuver

If the group of robots wish to pass through a narrow passageway a formation rotation may be necessary in order to avoid a collision. It is conceivable that this could happen while carrying a long 2×4 . In order to pass through a door the formation would have to rigidly rotate (see Figure 2).

While the application is different, the fundamental approaches to the coordination of multiple robot, spacecraft, and aircraft are very similar: the common theme being the coordination of multiple vehicles to accomplish an objective. There are roughly three approaches to multi-vehicle coordination reported in the literature, namely

- Leader-following,
- Behavioral, and
- Virtual structures [7].

In leader following, one of the robots is designated as the leader, with the rest of the robots designated as followers. The basic idea is that the followers track the position and

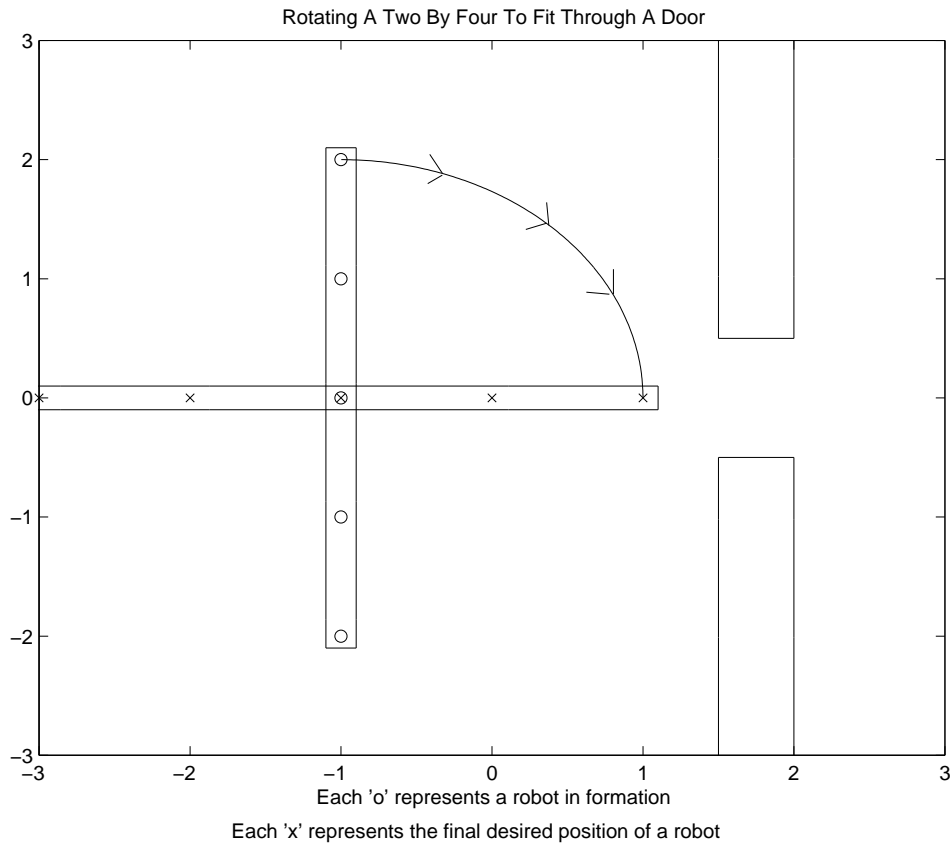


Fig. 2. Rotating A 2×4

orientation of the leader with some prescribed (possibly time-varying) offset. There are numerous variations on this theme including designating multiple leaders, forming a chain (robot i tracks robot $i - 1$), and other tree topologies.

One of the first studies on leader-following strategies is reported in [8] which discusses formation control laws for mobile robots. The application of these ideas to spacecraft formations is reported in [9], where explicit control laws for formation keeping and relative attitude alignment based on nearest neighbor-tracking are derived. Several leader-following techniques are discussed including leader tracking, nearest neighbor tracking, barycenter tracking, and other tree topologies. In [10], the ideas of [9] are extended to account for actuator saturation and are applied to the problem of controlling the formation to execute a continuous rotational slew. In [11], adaptive control laws are added to the control derived in [9] in order to reject common space disturbances.

There have been a number of studies of leader-following techniques in the mobile robotics

community. In [12], leader-following is used to control a group of mobile robots to cooperatively move a box. In [13], feedback linearization techniques are used to derive tracking control laws for nonholonomic robots that are used for leader-following. In addition, the authors describe the formation configuration as a directed graph. The shape of the formation is changed as graph structures are changed. Another approach to leader-following for multiple nonholonomic robots is described in [14].

The basic idea behind the behavioral approach is to prescribe several desired behaviors for each agent, and then to make the control action of each agent a weighted average of the control for each behavior. Possible behaviors include collision avoidance, obstacle avoidance, goal seeking, and formation keeping. There are also numerous variations on the behavioral approach to multi-agent coordination, most of which are derived by novel weightings of the behaviors.

In [15], the behavioral approach is applied to the problem of maintaining a constellation of satellites in an equally distributed ring formation in earth orbit. Simple Lyapunov control functions are used to maintain distance and avoid collisions. The application of the behavioral approach to aircraft flying in formation is described in [16], where the control strategies are derived to mimic the instinctive behavior of birds and fish. A paper that describes the behavioral approach to formation keeping for mobile robots is [17] where control strategies are derived by averaging several competing behaviors including goal seeking, collision avoidance, formation maintenance. Unit-center tracking, leader tracking and nearest neighbor tracking controls are also studied. In [18], the behavioral approach is used to cause a group of robots to create line and circle formations. These ideas are extended in [19] to the problem of controlling a formation of mobile robots to transport objects.

In the virtual structure approach, the entire formation is treated as a single structure. For example, in an interferometry mission it may be desirable to have a constellation of spacecraft act as a single rigid body. In the virtual structure approach, the control is derived in three steps: first, the desired dynamics of the virtual structure are defined, second, the motion of the virtual structure is translated into the desired motion for each agent, and finally, tracking controls for each spacecraft are derived.

The virtual structure approach can be implemented as a leader-following control. We treat the N robots in the formation as followers and then designate one “virtual” robot as a leader. Choosing the dynamics of the virtual robot to evolve as a second order system, we can choose the way that the formation evolves over time by appropriately picking the system parameters of the virtual leader.

The virtual structure approach was applied to formations of mobile robots in [20]. The application to formations of spacecraft in free space is described in [21], [22].

Leader-following, behavioral, and virtual structure approaches to the coordination problem have their corresponding strengths and weakness. The strength of leader-following is that group behavior is directed by specifying the behavior of a single quantity: the leader. The weakness, however, is that there is no explicit feedback to the formation. For example, the leader may be moving too fast for the following agents to track. Another weakness is that the leader is a single point of failure for the formation. For leader-following formation convergence depends on each follower knowing the position, velocity and acceleration of the leader. If this information is not available, then no convergence can be guaranteed. This renders a large communication burden for the the leader-following approach. Furthermore, due to communication latency and communication delays each robot will have to figure out what the leader is doing with old information that it receives only every couple of seconds.

The strength of the virtual structure approach is that it is fairly easy to prescribe a coordinated behavior for the group. The disadvantage is that requiring the formation to act as a virtual structure limits the class of potential applications of this approach. Another disadvantage is that in its current development the virtual structure approach lends itself to a centralized control implementation. This increases the communication burden to a higher order beyond that of the leader-following approach.

The strength of the behavioral approach is that it is natural to derive control strategies when agents have multiple competing objectives. In addition, there is explicit feedback to the formation since each agent reacts according to the position of its neighbors. Another strength is that the behavioral approach lends itself naturally to a decentralized implementation. The primary weakness is that group behavior cannot be explicitly defined, rather

the group behavior is said to “emerge.” Another weakness is that behavioral approaches are difficult to analyze mathematically and characteristics of the formation (like stability) cannot generally be guaranteed.

In this paper we will implement our control on a group of Hilare-type nonholonomic robots. In the well know paper by Brockett [23] it is shown that nonholonomic dynamics cannot be stabilized using time invariant continuous control. However, there exists several discontinuous control results for stabilizing a nonholonomic robot both for the kinematic set of equations [24], [25] and for the dynamic set of equations [24]. Furthermore this problem has also been solved using time-varying control laws. Many time-varying controls excite the robot dynamics with a periodic signal. The resultant trajectories are oscillatory in nature [26]. Another class of time-varying control that gets better results is hybrid control. Hybrid controls for this problem are presented in [27].

For the formation control problem in the nonholonomic domain, leader-following and virtual structure based control require that each follower robot track the motion of a leader robot. Although, work has been done on nonholonomic tracking [28], these controls are only convergent so long as the reference trajectory keeps on moving. Unfortunately, a large class of formation control problems require the group of robots to eventually stop.

In this paper we choose to take a different approach to controlling the nonholonomic robots in our formation. Control of Hilare-type robots is nonholonomic when we wish to control the center point of the robot to a particular position and orientation. However, the problem is no longer nonholonomic in nature when we choose to control an off-axis point with no control of the orientation. In fact, we show in this paper that it is feedback linearizable to a double integrator system. This has application to problems where off-axis grippers or sensors are to be maintained in formation.

The objective of this paper is to introduce the coupled dynamics approach to formation control. This approach is a behavioral formation control. However, our results provide a more rigorous analysis of the formation keeping and convergence than previously presented. Furthermore, this approach has the advantage that it can be implemented when only neighbor position information is available. This significantly cuts down the communication burden that plagues formation control.

In this paper we also define the concept of an Elementary Formation Maneuver (EFM). We decompose complex formation motion into a series of EFMs. A prior knowledge of the EFM that is to be implemented can also be used to significantly cut down on the required communication burden. We use the coupled dynamics approach to implement each of these EFMs.

In Section II we define the class of EFMs for the Robot Formation problem, and show that each of these maneuvers can be transformed into a rigid body formation translation of a double integrator system. In Section III we present the following coupled dynamics controls.

- The coupled dynamics control. This control uses the global and relative position of each robot to move the robot formation from one position to another, while maintaining the robots in formation during the maneuver. In the absence of relative velocity information, the relative motion among robots can be oscillatory when controlled by the coupled dynamics approach. The next control law addresses this concern
- The coupled dynamics control with passivity-based inter-agent damping. This control injects passivity based damping to the inter-robot motion. This significantly cuts down on the inter-robot oscillations.
- The coupled dynamics control with saturated control inputs. This final result is primarily of theoretical significance. All robots are subject to actuator saturation. We show that stability results are still possible even when the robot actuators are saturated.

In Section IV we present our simulation and hardware results. Section V gives our conclusions.

II. ELEMENTARY FORMATION MANEUVERS

A large class of complex formation motion can be realized as a succession of elementary formation maneuvers. In this paper we will realize the following maneuvers:

- Fixed Formation Translations,
- Fixed Formation Rotations,
- Formation Expansions (Contractions).

We implement this motion on a group of nonholonomic robots, each with the following equations of motion:

$$\begin{aligned}
 \dot{x} &= v \cos(\theta) \\
 \dot{y} &= v \sin(\theta) \\
 \dot{\theta} &= \omega \\
 \dot{v} &= \frac{F}{m} \\
 \dot{\omega} &= \frac{\tau}{J},
 \end{aligned} \tag{1}$$

where (x, y) is the Cartesian position of the robot, θ is the orientation of the robot, v is the tangential velocity of the robot, ω is the angular velocity, τ is the torque input, F is the force input, m is the mass and J is the moment of inertia.

In this paper we are interested in controlling an off axis point (x_h, y_h) located a length L in front of the robot, to maintain it in formation with similar points on other robots. This position is given by the equations

$$\begin{aligned}
 x_h &= x + L \cos(\theta) \\
 y_h &= y + L \sin(\theta).
 \end{aligned}$$

By controlling the motion of the point (x_h, y_h) the problem ceases to be nonholonomic. This problem was addressed for regulation with a kinematic control in [27]. We extend this result to the dynamic problem. We use feedback linearization to derive double integrator equations of motion for any elementary formation motion i.e. formation translations, formation expansions and formation rotations.

A. Formation Translations

For formation translations there exists a trade-off between maintaining formation and arriving at a final goal. Consider the example shown in Figure 3. The left triangle represents the desired formation for the group of robots at the initial time t_1 . Each vertex being a desired robot position. The right triangle represents the desired formation of the robots at time t_2 . Each 'x' represents the actual initial position of each robot. In this example a group of three robots are to move in formation to the right. However, one of

the robots begins the maneuver out of formation. In order to correct this problem it has two conflicting objectives:

- move right to arrive at the final goal,
- move left to regain formation.

If it moves left it will likely overshoot the formation, which is moving right, and if it moves right it will take longer to regain formation as the others “catch up”.

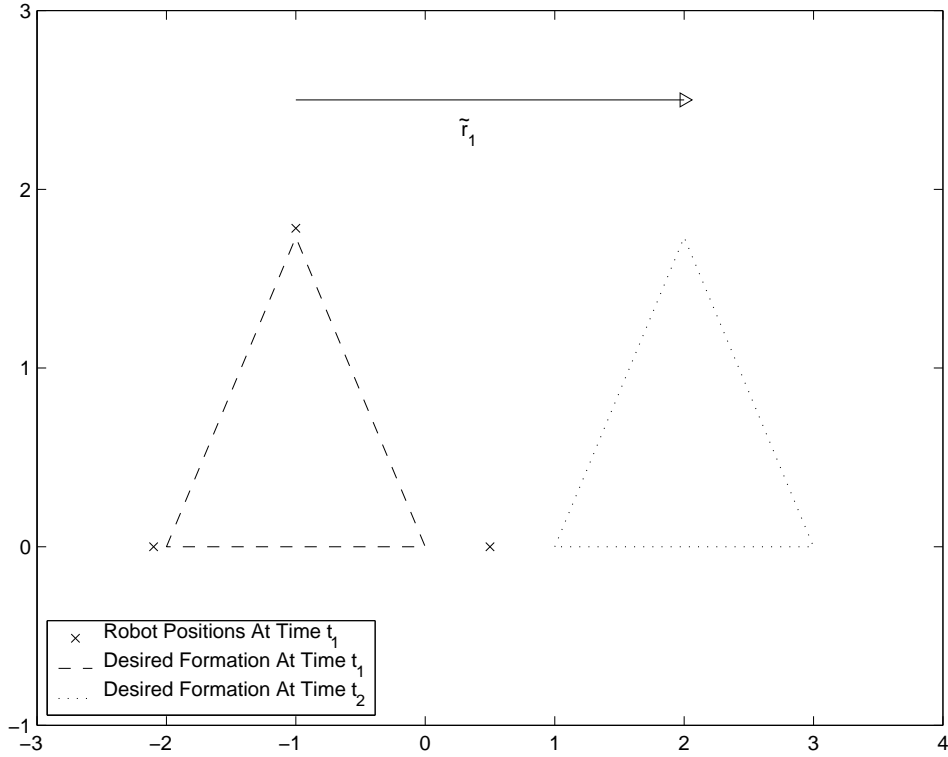


Fig. 3. Bottom right member of the formation is initially too far to the right

The coupled dynamics approach incorporates both of these competing objectives into the final control law. Suppose that we wish to implement a formation control on a group of N robots. Create two different error functions that each express one of these these competing objectives. First we develop an error function E_G that expresses the distance to arrive at the final goal, let

$$E_G = \sum_{i=1}^N \tilde{r}_i^T \tilde{r}_i,$$

where $r_i = (x_{hi}, y_{hi})^T$, $r_{id} = (x_{hid}, y_{hid})^T$ and $\tilde{r}_i = r_i - r_{id}$ (see Figure 3).

Next, let the error function E_F express how well the group of robots are keeping formation, where E_F is defined as

$$E_F = \sum_{i=1}^N (\tilde{r}_i - \tilde{r}_{i+1})^T (\tilde{r}_i - \tilde{r}_{i+1}),$$

and where the robot index is defined mod N i.e. $\tilde{r}_{N+1} = \tilde{r}_1$. By maintaining the quantity E_F small during the entire maneuver, the robots will equalize the distance that they need to go to reach the final goal. Note that $E_F = 0$ if and only if $\tilde{r}_i = \tilde{r}_{i+1}$ for all i . This is equivalent to saying that $r_i - r_{i+1} = r_{id} - r_{i+1,d}$. This will only be true if the robots are in the same relative formation that they will have at the end of the maneuver. Therefore when $E_F = 0$, the robots will be keeping formation, but they will not necessarily be at their final desired position.

We can now define a total error for the formation problem as a weighted sum of E_G and E_F

$$E = k_F E_F + k_G E_G, \quad (2)$$

where k_F and k_G weight the relative importance of formation keeping versus convergence.

The control objective is to cause $E \rightarrow 0$ asymptotically. To implement our control on nonholonomic robots, we will feedback linearize the system to get double integrator dynamics. The problem with feedback linearization is that often times “inverting the dynamics” requires a great deal of control effort. For the time being we will assume that we have sufficient control effort to do this. In Section III-C we show that convergence results are still obtainable in the presence of saturation.

To feedback linearize system (1), differentiate the vector (x_h, y_h) twice to get

$$\begin{bmatrix} \ddot{x}_h \\ \ddot{y}_h \end{bmatrix} = R(\theta) \begin{bmatrix} \frac{F}{M} - L\omega^2 \\ \frac{\tau L}{J} + v\omega \end{bmatrix}, \quad (3)$$

where

$$R(\theta) = \begin{bmatrix} \cos(\theta) & -\sin(\theta) \\ \sin(\theta) & \cos(\theta) \end{bmatrix}$$

Choosing

$$\begin{bmatrix} \frac{F}{M} \\ \frac{\tau L}{J} \end{bmatrix} = \begin{bmatrix} L\omega^2 \\ -v\omega \end{bmatrix} + R(-\theta) \begin{bmatrix} u_x \\ u_y \end{bmatrix}$$

gives

$$\begin{bmatrix} \ddot{x}_h \\ \ddot{y}_h \end{bmatrix} = \begin{bmatrix} u_x \\ u_y \end{bmatrix}. \quad (4)$$

Therefore the translation problem is to select a control law $u = (u_x, u_y)^T$ such that $E \rightarrow 0$ asymptotically.

B. Formation Expansions and Rotations

Formation Expansions and Rotations can be formulated as a formation translation in polar coordinates with translations along the radial axis corresponding to expansions, and translations along the polar axis corresponding to rotations. A polar plane translation in an arbitrary direction would be a spiral.

First we define the center of the coordinate system by the center of rotation or expansion, and express the robot positions in terms of polar coordinates

$$\begin{aligned} x_h &= \rho_h \cos(\phi_h) \\ y_h &= \rho_h \sin(\phi_h). \end{aligned} \quad (5)$$

Define the formation goal error by

$$E_G = \sum_{i=1}^N \left\{ \tilde{\rho}_{hi}^2 + \tilde{\phi}_{hi}^2 \right\},$$

and the formation keeping error by

$$E_F = \sum_{i=1}^N \left\{ (\tilde{\rho}_{hi} - \tilde{\rho}_{h,i+1})^2 + (\tilde{\phi}_{hi} - \tilde{\phi}_{h,i+1})^2 \right\},$$

where $\tilde{\rho}_{hi} = \rho_{hi} - \rho_{hid}$ and $\tilde{\phi}_{hi} = \phi_{hi} - \phi_{hid}$. Again let $E = k_F E_F + k_G E_G$. For example, if we pick $\rho_{hid} = \rho_{hi}$ and choose $\phi_{hid} = \phi_{hi} + \pi/4$, forcing $E \rightarrow 0$ will result in a formation rotation of $\frac{\pi}{4}$ radians. Alternatively letting $\rho_{hid} = \rho_{hi} + 5$ and $\phi_{hid} = \phi_{hi}$ will result in a

formation expansion by five units. Similarly if we vary both ϕ_{hi} and ρ_{hi} simultaneously, then the rotation will spiral outward.

In order to do formation rotations/expansions, we feedback linearize the robot dynamics in polar coordinates. Differentiating Equation (5) twice gives

$$\begin{bmatrix} \ddot{x}_h \\ \ddot{y}_h \end{bmatrix} = R(\phi_h) \begin{bmatrix} \ddot{\rho}_h - \rho_h \dot{\phi}_h^2 \\ \rho_h \ddot{\phi}_h + 2\dot{\phi}_h \dot{\rho}_h \end{bmatrix}. \quad (6)$$

Equating Equation (3) and Equation (6), we get that

$$R(\theta) \begin{bmatrix} \frac{F}{M} - L\omega^2 \\ \frac{\tau L}{J} + v\omega \end{bmatrix} = R(\phi_h) \begin{bmatrix} \ddot{\rho}_h - \rho_h \dot{\phi}_h^2 \\ \rho_h \ddot{\phi}_h + 2\dot{\phi}_h \dot{\rho}_h \end{bmatrix}.$$

Choosing

$$\begin{bmatrix} \frac{F}{M} \\ \frac{\tau L}{J} \end{bmatrix} = \begin{bmatrix} L\omega^2 \\ -v\omega \end{bmatrix} + R(\phi_h - \theta) \begin{bmatrix} u_\rho - \rho_h \dot{\phi}_h^2 \\ \rho_h u_\phi + 2\dot{\rho}_h \dot{\phi}_h \end{bmatrix}$$

renders the polar equations in double integrator form

$$\begin{bmatrix} \ddot{\rho}_h \\ \ddot{\phi}_h \end{bmatrix} = \begin{bmatrix} u_\rho \\ u_\phi \end{bmatrix}. \quad (7)$$

The formation rotation/expansion problem is of the same form as the formation translation problem. We need to force $E \rightarrow 0$ given the double integrator dynamics (7).

III. FORMATION CONTROL

Suppose that we have feedback linearized the dynamics of a system in a given coordinate frame $z_i \in \mathbb{R}^2$ to be double integrator dynamics

$$\ddot{z}_i = u_i, \quad (8)$$

where $u_i \in \mathbb{R}^2$. The objective is to translate the group of robots in rigid formation within this new coordinate frame. A rigid translation in the z frame will produce a final desired position for each robot of $z_{id} = z_{io} + \Delta z$, where z_{io} is the initial position of the i th robot and Δz is the desired change in coordinates for all of the robots. We can thus define the

distance to go to reach the final goal as $\tilde{z}_i = z_i - z_{id}$. For the general formation control problem we wish to have $\tilde{z}_i \rightarrow 0$ uniformly over i .

From the previous section, we see that the general formation control problem for an elementary formation maneuver (i.e. rotations/expansions or translations) can be stated as

$$\begin{aligned} E &= k_F E_F + k_G E_G \\ E_G &= \sum_{i=1}^N \tilde{z}_i^T \tilde{z}_i \\ E_F &= \sum_{i=1}^N (\tilde{z}_i - \tilde{z}_{i+1})^T (\tilde{z}_i - \tilde{z}_{i+1}) \end{aligned} \tag{9}$$

where $\{u_i\}_{i=1}^N$ is to be chosen such that $E \rightarrow 0$ asymptotically.

For the robot translation problem $z_i = (x_{hi}, y_{hi})^T$, and for the robot rotation problem $z_i = (\rho_{hi}, \phi_{hi})^T$. The double integrator dynamics are achieved by feedback linearizing the appropriate set of equations. We will take the following approaches to asymptotically stabilize E .

- The Coupled Dynamics Approach (described in Section III-A), which implements straight forward feedback on the global and relative positions of each robot,
- The Coupled Dynamics Approach with Passivity-Based Inter-Agent Damping (described in Section III-B) which additionally includes an inter-robot damping,
- The Coupled Dynamics Approach with Saturated Control (described in Section III-C) , shows that the couple dynamics approach still works when the control inputs are saturated.

A. Coupled Dynamics Formation Control

Theorem III.1 provides a formation control for a group of N nonholonomic robots. This control weights the two competing behaviors of convergence to the final goal, and formation keeping. By doing this the robots converge to their final desired position while equalizing the distance that each robot has yet to travel. This equalization allows all of the robot to stay in formation while completing the maneuver.

Theorem III.1: Given the system defined in Equation (8) and the error function defined

in equation (9), if

$$\begin{aligned} u_i &= -k_F(\tilde{z}_i - \tilde{z}_{i+1}) - k_F(\tilde{z}_i - \tilde{z}_{i-1}) - k_G\tilde{z}_i - d_F\dot{z}_i. \\ z_i(0) &= z_{i0} \\ \dot{z}_i(0) &= 0, \end{aligned} \tag{10}$$

and $k_F \geq 0, k_G > 0$ then $E(t) \rightarrow 0$ asymptotically and $E(t) \leq E(0) - \mathcal{D}(\dot{z}_i(t))$, where

$$\mathcal{D}(\dot{z}_i(t)) = \sum_{i=1}^N \dot{z}_i^T \dot{z}_i > 0.$$

The main idea of Control (10) is to drive each robot to its final desired position while maintaining the formation. The term in the control $-k_G\tilde{z}_i$ drives the i th robot to its final desired position. The two terms $-k_F(\tilde{z}_i - \tilde{z}_{i+1})$ and $k_F(\tilde{z}_i - \tilde{z}_{i-1})$ serve to equalize the distances $\tilde{z}_i, \tilde{z}_{i-1}$, and \tilde{z}_{i+1} . By equalizing these distances each robot is progressing to its goal at the same pace. This forces the robots to maintain formation during the entire maneuver. Additionally a conservative bound on the formation error $E(t)$ is the initial formation error $E(0)$. This means that while the robots are executing the EFM, the error will never be worse than the initial error. The additional quadratic function of the robot velocities $\mathcal{D}(\dot{z}_i)$ decreases the bound $E(t)$. The greater the velocities of the robots the greater the reduction.

Proof: Consider the function

$$V = \frac{1}{2}E + \frac{1}{2}\mathcal{D}(\dot{z}_i). \tag{11}$$

Differentiating we find that

$$\begin{aligned} \dot{V} &= \sum_{i=1}^N \dot{z}_i^T (k_G\tilde{z}_i + k_F(\tilde{z}_i - \tilde{z}_{i+1}) + k_F(\tilde{z}_i - \tilde{z}_{i-1}) + u_i) \\ &= -d_C \sum_{i=1}^N \dot{z}_i^T \dot{z}_i \\ &\leq 0. \end{aligned} \tag{12}$$

Since $\dot{V} \leq 0$ it follows that $V(t) \leq V(0)$ and

$$\begin{aligned}
E(t) + \mathcal{D}(t) &= 2V(t) \\
&\leq 2V(0) \\
&= E(0) + \mathcal{D}(0) \\
&= E(0) \\
&\Rightarrow \\
E(t) &\leq E(0) - \mathcal{D}(t)
\end{aligned}$$

We now show that $E(t) \rightarrow 0$. It is sufficient to show that $\tilde{z}_i \rightarrow 0$. Consider the set $\Omega = \{\tilde{z}_i, \dot{\tilde{z}}_i | \dot{V} = 0\}$. Let $\bar{\Omega}$ be the largest invariant set in Ω . From equation (12) when $\dot{V} = 0$ we have that $\dot{\tilde{z}}_i = 0$ and $u_i = 0$. From equation (10) $\tilde{z}_i \in \bar{\Omega}$ satisfies

$$(2k_F + k_G)\tilde{z}_i - k_F\tilde{z}_{i-1} - k_F\tilde{z}_{i+1} = 0. \quad (13)$$

This may be written in matrix form as

$$(C(k_G, k_F) \otimes I_2)\tilde{z} = 0, \quad (14)$$

where $C(k_G, k_F)$ is a circulant matrix with first row equal to $[k_G + 2k_F, -k_F, 0, \dots, 0, -k_F] \in \mathbb{R}^N$, $\tilde{z} = [\tilde{z}_1^T \dots \tilde{z}_N^T]^T$ and where \otimes is the Kronecker product. It follows that $\tilde{z} = 0$ if $C(k_G, k_F) \otimes I_3$ is nonsingular. The matrix $C(k_G, k_F) \otimes I_3$ is nonsingular if and only if $C(k_G, k_F)$ is nonsingular. Since $C(k_G, k_F)$ is a circulant matrix it can be unitarily diagonalized by a *DFT* matrix V [29]

$$C(k_G, k_F) = V^H D V,$$

where

$$\begin{aligned}
D &= (2k_F + k_G)I_N - k_F W - k_F W^{N-1}, \\
W &= \text{diag}(1, W_N^{-1}, \dots, W_N^{-(N-1)}), \\
W_N &= e^{j(2\pi/N)}.
\end{aligned}$$

Multiplying $W W^{N-1}$ we see that

$$W W^{N-1} = I_N$$

therefore we may write

$$\begin{aligned} W^{N-1} &= W^{-1} \\ &= \text{diag}(1, W_N, \dots, W_N^{N-1}). \end{aligned}$$

Thus

$$D = \text{diag}(2k_F + k_G, 2k_F(1 - \cos(2\pi/N)) + k_G, \dots, 2k_F(1 - \cos(2(N-1)\pi/N)) + k_G)$$

Therefore the eigenvalues of $C(k_G, k_F)$ are

$$\lambda_i(C(k_G, k_F)) = 2k_F(1 - \cos(2\pi(i-1)/N)) + k_G,$$

where $0 \leq i \leq N-1$. Since $k_F \geq 0$ and $k_G > 0$, $C(k_G, k_F)$ is nonsingular. ■

The simulation and hardware results for this problem will be found in Section IV.

B. Coupled Dynamics Formation Control With Passivity-Based Inter-Robot Damping

The only damping that is added to the Formation control is from the term \dot{z}_i . This damps the global motion of the i th robot but it does not damp out the inter-robot oscillations. Relative motion between the i th robot and its neighbors may be oscillatory despite smooth transitions to the goal. There are two approaches to removing this oscillatory behavior. The first would be to feedback the relative velocity of the i th robot with respect to one or more of its neighbors. The difficulty of this approach is the requirement that the i th neighbor would need to know the velocity of some of its neighbors. The other approach is to apply damping injection via the Passivity-Based-Control (PBC) approach [30], [31], [32]. This would only require that the i th robot have position information of its neighbors. This is the approach followed here. It is of interest to note that we could have used a PBC to damp out the quantity \tilde{z}_i . However, for the robot application, which requires velocity information to perform the feedback linearization, it is wise to use the velocity information since it is available.

Theorem III.2 provides a formation control for a group of N nonholonomic robots, using passivity based inter-robot damping. The only difference between this control and that presented in Theorem III.1 is the addition of the term γ_i which adds the inter-robot damping.

Theorem III.2: Given the feedback linearized dynamics from Equation (8) and the error functions in Equation (9), if

$$\begin{aligned}
u_i &= -k_F(\tilde{z}_i - \tilde{z}_{i+1}) - k_F(\tilde{z}_i - \tilde{z}_{i-1}) - k_G(\tilde{z}_i) - d\dot{z}_i - \gamma_i. \\
\dot{\xi}_i &= A\xi_i + d_G\tilde{z}_i + d_F(\tilde{z}_i - \tilde{z}_{i-1}) + d_F(\tilde{z}_i - \tilde{z}_{i+1}) \\
\gamma_i &= PA\xi_i + d_GP\tilde{z}_i + d_FP(\tilde{z}_i - \tilde{z}_{i-1} + d_F(\tilde{z}_i - \tilde{z}_{i+1})) \\
\xi_i(0) &= -A^{-1}(d_G\tilde{z}_i(0) + d_F(\tilde{z}_i(0) - \tilde{z}_{i-1}(0)) \\
&\quad + d_F(\tilde{z}_i(0) - \tilde{z}_{i+1}(0))) \\
z_i(0) &= z_{io} \\
\dot{z}_i(0) &= 0,
\end{aligned} \tag{15}$$

- $k_F, d_F, d \geq 0, k_G, d_G > 0,$
- A is Hurwitz
- $P = P^T > 0$ is the solution to $A^T P + P A^T = -Q,$ where $Q > 0.$

then $E(t) \rightarrow 0$ asymptotically and $E(t) \leq E(0) - \mathcal{D}(\dot{z}(t)) - \mathcal{P}(\dot{\xi}(t)),$ where

$$\mathcal{D}(\dot{z}(t)) = \sum_{i=1}^N \dot{z}_i^T \dot{z}_i$$

$$\mathcal{P}(\dot{\xi}(t)) = \dot{\xi}^T (D^{-1} \otimes P) \dot{\xi} > 0,$$

$\xi = [\xi_1^T, \xi_2^T, \dots, \xi_N^T]^T,$ and where $D = \text{circ}(2d_F + d_G, -d_G, 0, \dots, 0, -d_G) = D^T > 0.$ The error $E(t)$ can still be conservatively bound from above by the initial error $E(0).$ In the case of the passivity based coupled dynamics control, this bound is lowered by the two quadratic functions $\mathcal{D}(\dot{z}(t))$ and $\mathcal{P}(\dot{\xi}(t)).$ The greater the velocity terms \dot{z}_i and $\dot{\xi}_i$ the lower the bound on $E(t).$

Proof: Let

- $z = [z_1^T, z_2^T, z_3^T, \dots, z_N^T]^T$
- $\tilde{z} = [\tilde{z}_1^T, \tilde{z}_2^T, \tilde{z}_3^T, \dots, \tilde{z}_N^T]^T$
- $\gamma = [\gamma_1^T, \gamma_2^T, \gamma_3^T, \dots, \gamma_N^T]^T$
- $\xi = [\xi_1^T, \xi_2^T, \xi_3^T, \dots, \xi_N^T]^T.$

and let $D = \text{circ}(2d_F + d_G, -d_G, 0, \dots, 0, -d_G)$ be a circulant matrix, where the arguments of circ correspond to the first row of the circulant matrix. Note that from the proof of

Theorem III.1 we showed that eigenvalues of D are all greater than zero since $d_F \geq 0$ and $d_G > 0$. Furthermore it can be observed that $D = D^T > 0$. It is also true that $D^{-1} = D^{-T} > 0$. Also let $K = \text{circ}(2k_F + k_G, -k_G, 0, \dots, 0, -k_G) = K^T > 0$

Given these definitions we can write the control from Equation (15) as

$$\begin{aligned} u &= -Kz - \gamma - d\dot{z} \\ \dot{\xi} &= (I_N \otimes A)\xi + (D \otimes I_n)\tilde{r} \\ \gamma &= (I_N \otimes PA)\xi + (D \otimes P)\tilde{r}, \end{aligned} \tag{16}$$

where \otimes is the Kronecker product operator [33].

Consider the Lyapunov function candidate

$$V = \frac{1}{2}E + \frac{1}{2}\dot{r}^T\dot{r} + \frac{1}{2}\xi^T(D^{-1} \otimes P)\xi. \tag{17}$$

It is of interest to note that $D^{-1} \otimes P = (D^{-1} \otimes P)^T > 0$. Which implies that V is a positive definite function. This follows from the fact that the Kronecker product of two positive definite symmetric matrices is positive definite and symmetric [33].

Differentiating both sides of equation (17) we arrive at

$$\dot{V} = \dot{z}^T(u + K\tilde{z} + \gamma) - \frac{1}{2}\dot{\xi}(D^{-1} \otimes Q)\dot{\xi}.$$

Substituting in control (16) gives

$$\begin{aligned} \dot{V} &= -d\dot{z}^T\dot{z} - \frac{1}{2}\dot{\xi}(D^{-1} \otimes Q)\dot{\xi} \\ &\leq 0 \end{aligned}$$

Now we will show that $E(t) \rightarrow 0$ asymptotically. Again it is sufficient to show that $\tilde{z} \rightarrow 0$ asymptotically. Let $\Sigma = \{\tilde{z}, \dot{z} | \dot{V} = 0\}$ and let $\bar{\Sigma}$ be the largest invariant subset of Σ . When $\dot{V} = 0$, $\dot{z} = u = \dot{\xi} = 0$. Since, from (16) $\gamma = (I_N \otimes P)\dot{\xi}$ and P is full rank, $\gamma = 0$. From equation (16) when $\dot{z} = \gamma = u = 0$,

$$K\tilde{z} = 0.$$

In the proof of Theorem III.1 we showed that K is full rank. Therefore $\tilde{z} = 0$ and $\bar{\Sigma} = \{0, 0\}$. Hence by LaSalle's invariance principle $\tilde{z} \rightarrow 0$ asymptotically. ■

C. Saturated Control

The results of Theorem III.1 and Theorem III.2 work well executing Elementary Formation Maneuvers even in the presence of actuator saturation. However, they do not guarantee convergence in the presence of saturation. By implementing a control that explicitly takes saturation into account we can show convergence even in the presence of saturation.

The saturation control problem appends an additional constraint to Equation (1).

$$\begin{aligned} |F| &\leq F_{Max} \\ |\tau| &\leq \tau_{Max}, \end{aligned}$$

where the typical saturation bound for the robots used in our testbed are $F_{Max} = 30N$ and $\tau_{Max} = 230Nm$. Unfortunately, these saturation bounds cannot be applied directly to the feedback linearized dynamics (8) since the feedback linearization explicitly depends on the tangential and angular velocity of each robot. However, since each EFM involves moving the robot only a finite distance we can assume, that given the bounded acceleration of the system, the robot velocity will also be bounded. Therefore, we can derive a bound on the feedback linearized forces

$$\|u_z\| \leq u_{max}$$

For the saturated control problem we wish to choose our error functions such that the error only grows linearly rather than quadratically as in the case of the previous section. Therefore we will select

$$\begin{aligned} E_G &= \sum_{i=1}^N \sum_{j=1}^2 \frac{1}{k} \log(\cosh(k\tilde{z}_{ij})) \\ E_F &= \sum_{i=1}^N \sum_{j=1}^2 \frac{1}{k} \log(\cosh(k(\tilde{z}_{ij} - \tilde{z}_{i+1,j}))), \end{aligned} \tag{18}$$

where

$$\tilde{z}_i = \begin{bmatrix} \tilde{z}_{i1} \\ \tilde{z}_{i2} \end{bmatrix}$$

We choose our total formation error as the weighted sum of E_F and E_G i.e.

$$E = k_F E_F + k_G E_G.$$

Theorem III.3 presents results similar to Theorem III.1 but using saturated control inputs.

Theorem III.3: Given the feedback linearized dynamics (8) and the error function (18), if

$$\begin{aligned} u_i &= -k_F \tanh(k(\tilde{z}_i - \tilde{z}_{i+1})) - k_F \tanh(k(\tilde{z}_i - \tilde{z}_{i-1})) \\ &\quad - k_G \tanh(k\tilde{z}_i) - d \tanh(k\dot{z}_i) \\ \dot{z}_i(0) &= 0 \\ z_i(0) &= z_i o \end{aligned} \tag{19}$$

where

$$\tanh \left(\begin{bmatrix} x \\ y \end{bmatrix} \right) = \begin{bmatrix} \tanh(x) \\ \tanh(y) \end{bmatrix},$$

$k_F \geq 0$ and $k_G, k, d > 0$ then

1. $\|u_i\|_\infty \leq k_G + d + 2k_F$
2. $\forall t \geq 0, E(t) \leq E(0) - \frac{1}{2}\mathcal{D}(\dot{z}_i(t))$ where

$$\mathcal{D} = \sum_{i=1}^N \dot{z}_i^T \dot{z}_i$$

3. $E(t) \rightarrow 0$ asymptotically

Proof:

1. Since each component of \tanh is bounded by one, each component of the control will be bounded by $k_G + d + 2k_F$. Therefore $\|u_i\|_\infty \leq k_G + d + 2k_F$.
2. Consider the Lyapunov function candidate

$$V = E + \frac{1}{2}\mathcal{D}(\dot{z}_i(t))$$

Differentiating, we get that

$$\begin{aligned}
\dot{V} &= k_F \sum_{i=1}^N \sum_{j=1}^2 (\tanh(k(\tilde{z}_{ij} - \tilde{z}_{i+1,j})))(\dot{z}_{ij} - \dot{z}_{i+1,j}) \\
&\quad + k_G \tanh(k\tilde{z}_{ij}) \dot{z}_{ij} \dot{z}_{ij}^T u_{ij} \\
&= \sum_{i=1}^N \dot{z}_i^T (u_i + k_F \tanh(k(\tilde{z}_i - \tilde{z}_{i+1}))) \\
&\quad + k_F \tanh(k(\tilde{z}_i - \tilde{z}_{i-1})) + k_G \tanh(k\tilde{z}_i).
\end{aligned}$$

By equation (19) and the fact that the components of \tanh are odd functions it follows that

$$\dot{V} = -d \sum_{i=1}^N \dot{z}_i^T \tanh(k\dot{z}_i) \leq 0. \quad (20)$$

Thus V is a Lyapunov function and $V(\tilde{z}_i(0)) \geq V(\tilde{z}_i(t))$. Since $\dot{z}_i(0) = 0$,

$$\begin{aligned}
E(t) + \frac{1}{2} \mathcal{D}(\dot{z}_i(t)) &= V(t) \\
&\leq V(0) \\
&= E(0) \\
&\Rightarrow \\
E(t) &\leq E(0) - \frac{1}{2} \mathcal{D}(\dot{z}_i(t))
\end{aligned}$$

3. Since V is a Lyapunov function we can use LaSalle's invariance principle to show convergence. Let $\Sigma = \{\tilde{z}_i, \dot{z}_i | \dot{V} = 0\}$. Furthermore let $\bar{\Sigma}$ be the largest invariant set contained in Σ . When $\dot{V} = 0$ it follows from equation (20) that $\dot{z}_i = 0$ and $u_i = 0$. Thus from equation (19) we get

$$k_F \tanh(k(\tilde{z}_i - \tilde{z}_{i+1})) + k_f \tanh(k(\tilde{z}_i - \tilde{z}_{i-1})) + k_G \tanh(k\tilde{z}_i) = 0.$$

Alternatively we may write this as

$$\begin{aligned}
(k_G + 2k_F) \tanh(k\tilde{z}_i) + k_F (\tanh(k(\tilde{z}_i - \tilde{z}_{i+1})) - \tanh(k\tilde{z}_i)) \\
+ k_F (\tanh(k(\tilde{z}_i - \tilde{z}_{i-1})) - \tanh(k\tilde{z}_i)) = 0,
\end{aligned}$$

or broken into individual components as

$$\begin{aligned}
(k_G + 2k_F) \tanh(k\tilde{z}_{i1}) &+ k_F(\tanh(k(\tilde{z}_{i1} - \tilde{z}_{i+1,1})) - \tanh(k\tilde{z}_{i1})) & (21) \\
&+ k_F(\tanh(k(\tilde{z}_{i1} - \tilde{z}_{i-1,1})) - \tanh(k\tilde{z}_{i1})) = 0 \\
(k_G + 2k_F) \tanh(k\tilde{\gamma}_i) &+ k_F(\tanh(k(\tilde{z}_{i2} - \tilde{z}_{i+1,2})) - \tanh(k\tilde{z}_{i2})) \\
&+ k_F(\tanh(k(\tilde{z}_{i2} - \tilde{z}_{i-1,2})) - \tanh(k\tilde{z}_{i2})) = 0.
\end{aligned}$$

Note that since \tilde{z}_{i1} and \tilde{z}_{i2} satisfy the same form of equation it is only necessary to show that $\tilde{z}_{i1} \rightarrow 0$.

To show this we will apply the identity (see [34])

$$\tanh(u) - \tanh(v) = \frac{\sinh(u - v)}{\cosh(u) \cosh(v)}$$

to equation (21) to get

$$\begin{aligned}
(k_G + 2k_F) \sinh(k\tilde{z}_{i1}) - k_F \operatorname{sech}(k(\tilde{z}_{i1} - \tilde{z}_{i+1,1})) \sinh(k\tilde{z}_{i+1,1}) \\
- k_F \operatorname{sech}(k(\tilde{z}_{i1} - \tilde{z}_{i-1,1})) \sinh(k\tilde{z}_{i-1,1}) = 0.
\end{aligned}$$

Now we may write this system of equations in matrix form as

$$((k_G + 2k_F)I_N + B) \begin{pmatrix} \sinh(k\tilde{z}_{11}) \\ \sinh(k\tilde{z}_{21}) \\ \vdots \\ \sinh(k\tilde{z}_{N1}) \end{pmatrix} = 0, \quad (22)$$

where

$$\begin{aligned}
B = -k_F \sum_{i=1}^N (e_i e_{i+1}^T \operatorname{sech}(k(\tilde{z}_{i1} - \tilde{z}_{i+1,1})) \\
+ e_i e_{i-1}^T \operatorname{sech}(k(\tilde{z}_{i1} - \tilde{z}_{i-1,1}))).
\end{aligned}$$

Since $\sinh(k\tilde{z}_{i1}) = 0$ if and only if $\tilde{z}_{i1} = 0$ to prove that $\tilde{z}_{i1} \rightarrow 0$ for all i it is sufficient to show that $(k_G + 2k_F)I_N + B$ is full rank.

To do this let us calculate the induced two norm $\|B\|_2$. Let $w = \sum_{j=1}^N w_j e_j$ be an arbitrary

non-zero vector.

$$\begin{aligned}
\|Bw\|_2 &= k_F \left\| \sum_{i=1}^N (e_i e_{i+1}^T \operatorname{sech}(k(\tilde{z}_{i1} - \tilde{z}_{i+1,1})))w \right. \\
&\quad \left. + \sum_{i=1}^N e_i e_{i-1}^T \operatorname{sech}(k(\tilde{z}_{i1} - \tilde{z}_{i-1,1}))w \right\|_2 \\
&\leq k_F \left\| \sum_{i=1}^N (e_i e_{i+1}^T \operatorname{sech}(k(\tilde{z}_{i1} - \tilde{z}_{i+1,1})))w \right\| \\
&\quad + \left\| \sum_{i=1}^N e_i e_{i-1}^T \operatorname{sech}(k(\tilde{z}_{i1} - \tilde{z}_{i-1,1}))w \right\|_2 \\
&= k_F \left\| \sum_{i=1}^N \sum_{j=1}^N (e_i e_{i+1}^T e_j w_j \operatorname{sech}(k(\tilde{z}_{i1} - \tilde{z}_{i+1,1}))) \right\| \\
&\quad + k_F \left\| \sum_{i=1}^N \sum_{j=1}^N e_i e_{i-1}^T e_j w_j \operatorname{sech}(k(\tilde{z}_{i1} - \tilde{z}_{i-1,1})) \right\|_2 \\
&= k_F \left\| \sum_{i=1}^N \sum_{j=1}^N (e_i \delta_{i+1,j} w_j \operatorname{sech}(k(\tilde{z}_{i1} - \tilde{z}_{i+1,1}))) \right\| \\
&\quad + k_F \left\| \sum_{i=1}^N \sum_{j=1}^N e_i \delta_{i-1,j} w_j \operatorname{sech}(k(\tilde{z}_{i1} - \tilde{z}_{i-1,1})) \right\|_2 \\
&= k_F \left\| \sum_{i=1}^N (e_i w_{i+1} \operatorname{sech}(k(\tilde{z}_{i1} - \tilde{z}_{i+1,1}))) \right\| \\
&\quad + k_F \left\| \sum_{i=1}^N e_i w_{i-1} \operatorname{sech}(k(\tilde{z}_{i1} - \tilde{z}_{i-1,1})) \right\|_2 \\
&= k_F \sqrt{\sum_{i=1}^N w_{i+1}^2 \operatorname{sech}(k(\tilde{z}_{i1} - \tilde{z}_{i+1,1}))^2} \\
&\quad + k_F \sqrt{\sum_{i=1}^N w_{i-1}^2 \operatorname{sech}(k(\tilde{z}_{i1} - \tilde{z}_{i-1,1}))^2} \\
&\leq k_F \sqrt{\sum_{i=1}^N w_{i+1}^2} + k_F \sqrt{\sum_{i=1}^N w_{i-1}^2} \\
&= 2k_F \|w\|.
\end{aligned}$$

Since our choice of w was arbitrary it follows that the induced two norm

$$\|B\|_2 \leq 2k_F.$$

Since $(k_G + 2k_F)I_N$ is non-singular with minimum singular value $\underline{\sigma}((k_G + 2k_F)I_N) = k_G + 2k_F$, and since the maximum singular value of B is $\bar{\sigma} \leq 2k_F$ then a sufficient condition for $(k_G + 2k_F)I_N + B$ to be full rank is to have $k_G + 2k_F > 2k_F$. This is always true since $k_G > 0$. ■

IV. SIMULATION AND HARDWARE RESULTS

A. Simulation Results

The simulation results for translation, rotation and expansion are similar. Here we give simulations for the robot formation rotation case. For this problem we will assume that the robots begin in a circular formation. The nominal system parameters for each robot is $J = .69Kg\,m^2$ and $m = 8.22Kg$, these are the approximate parameters of the robots in our test-bed. Furthermore we assume that the robots are initially out of formation with a zero mean formation error on x, y of variance $0.1m^2$ and zero mean formation error on θ with a variance of $0.1rad^2$ for each robot. Furthermore, we assume that parameter uncertainty error for each robot is zero mean with variance $0.25 Kg^2$ on the masses and variance $0.25 Kg^2/m^2$ on the moment of inertia. In addition we have included actuator saturation effects in the simulations. These saturation values are based on the actual testbed. The torque saturates at $230Nm$ and the force saturates $30N$.

For each of the simulations we include five plots. These plots contain global and relative position information for the first robot. The first plot displays the global error term \tilde{z}_1 for the first robot. Convergence in this variable shows convergence to the final goal of the robot. The remaining four plots display relative position information. These plots display the function $\|\tilde{z}_1 - \tilde{z}_i\|$ for $i = 1, 2, 3, 4$. In simulation it is observed that five identical well modeled robots that begin in perfect formation will remain in perfect formation during an entire simulation if they are controlled by the same coupled dynamics control law. This follows from uniqueness properties of solutions of ordinary differential equations. In order

to put the formation control algorithm to a real test in simulation modeling errors and initial formation errors are included.

In the first simulation (Figure 4 dashed line) the robots only coordinate the time that they start the maneuver. There is not coordination of the relative robot positions. We set $k_G = 1$, $d = 2$ and $k_F = 0$.

In the second simulation (Figure 4 dotted line) using the results of Theorem III.1 we add a feedback term of $k_F = 20$ on the relative formation keeping errors of the robots. This significantly improves the formation keeping during the rotation at the expense of more oscillations in the relative motions. As mentioned previously these oscillations could be damped out if the relative velocity of pairs of robots were known. However, in the absence of this knowledge, we add in a passivity-based control term. This significantly damps out the oscillations that exist in the relative motion of the robots (Figure 4 solid line).

In the third simulation we use the following parameters: $d_F = 100$, $d_C = 10$, $A = -100I_2$ and $Q = 200I_2$.

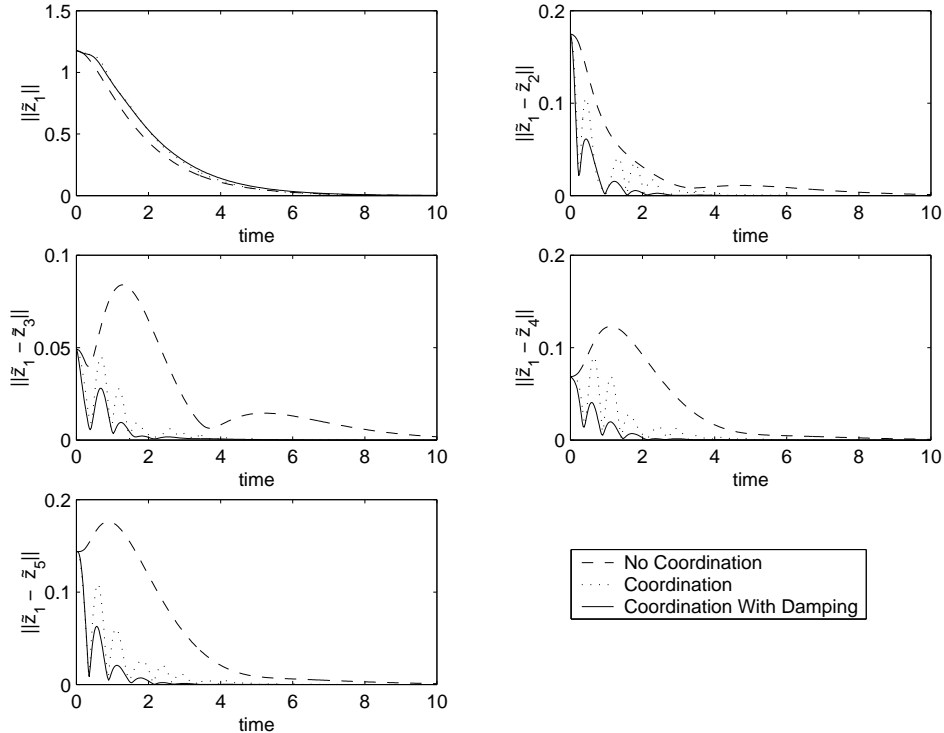


Fig. 4. Simulation Plot of First Robot's Formation Errors.

It is clear that the overall convergence of each robot in these simulations is almost identical in each of the three cases. However, there is drastic improvement in the relative robot motion as we progress through the three different simulations. In the first example there is a large overshoot in the relative robot motion. This is an obvious result of not having any coordination between the different agents. By adding relative motion feedback this overshoot is almost entirely eliminated at the expense of some oscillatory behavior in the relative robot motion. Finally using Theorem III.2 we add the PBC inter-agent damping term to significantly attenuate the amplitude of the inter-robot oscillations.

We will present one final simulation which illustrates the results of Theorem III.3. In this example we use the following parameters: $d = 2$, $k_F = 20$, and $k_G = 1$. Figure 5 gives the plots of the first robot relative to the final goal and relative to the motion of the four other robots.

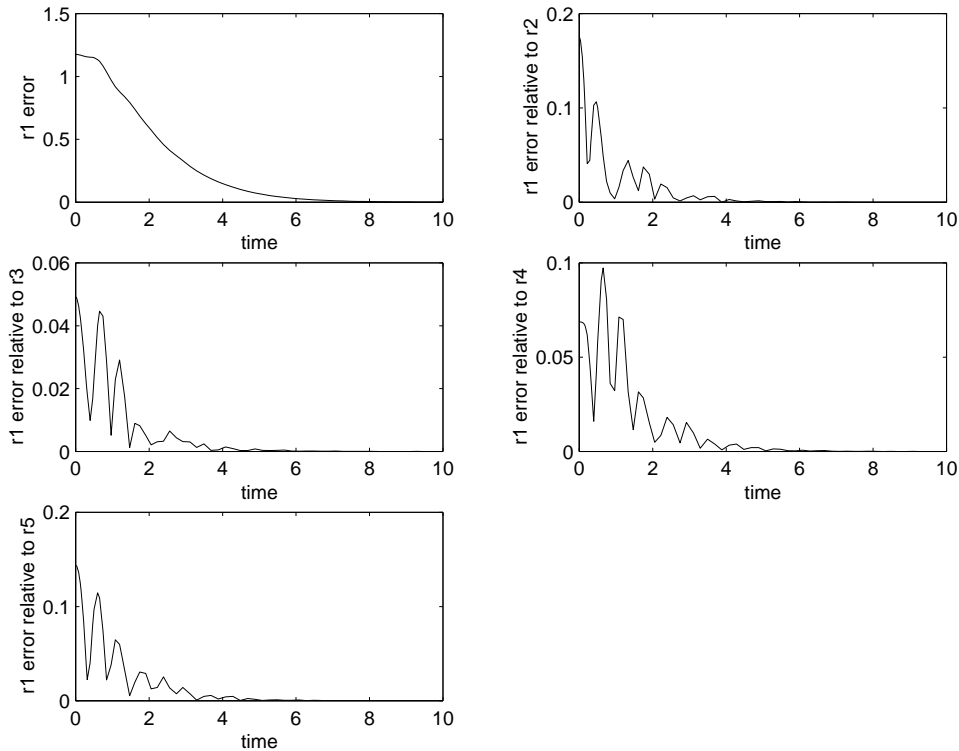


Fig. 5. Simulation Plot of First Robot Errors With Saturated Relative Motion Feedback.

In the next section we take these same results and implement them in our hardware testbed.

B. Hardware Results

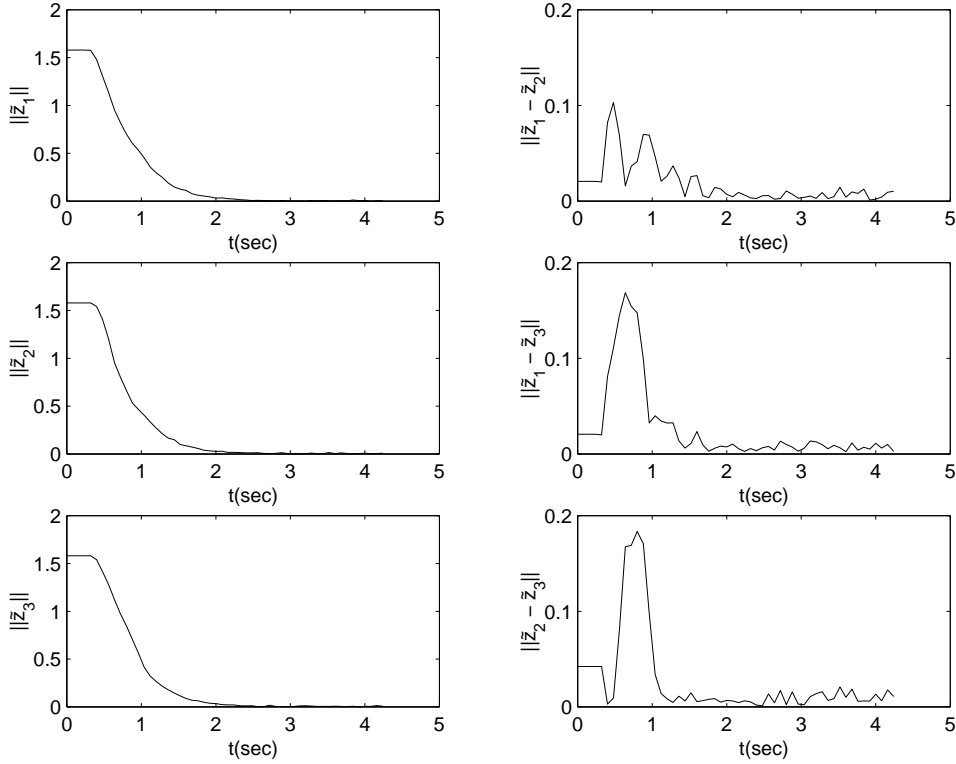


Fig. 6. Hardware Results: Relative position Errors For Each Robot.

We implemented the results of Theorem III.1 for a formation rotation on a group of three robots. The robots begin the maneuver with the group of robots in perfect formation. They are then to move so as to rotate the formation rigidly 90° . Figure 6 plots the global robot errors $\|\tilde{z}_i\|$ and the relative position errors $\|\tilde{z}_i - \tilde{z}_j\|$ for each pair of robots as a function of time. Finally, Figure 7 shows the global trajectory of each robot. It is apparent from the plot the overall convergence of the formation control. It is also observed that formation keeping errors are kept small during the course of the maneuver.

V. CONCLUSIONS

In this paper we introduced the concept of Elementary Formation Maneuvers (EFMs). EFMs are a class of formation maneuvers that preserve the shape of the formation. Included in this class of maneuvers are formation rotations, expansions/contractions and translations. We specifically considered these three maneuvers since more complex mo-

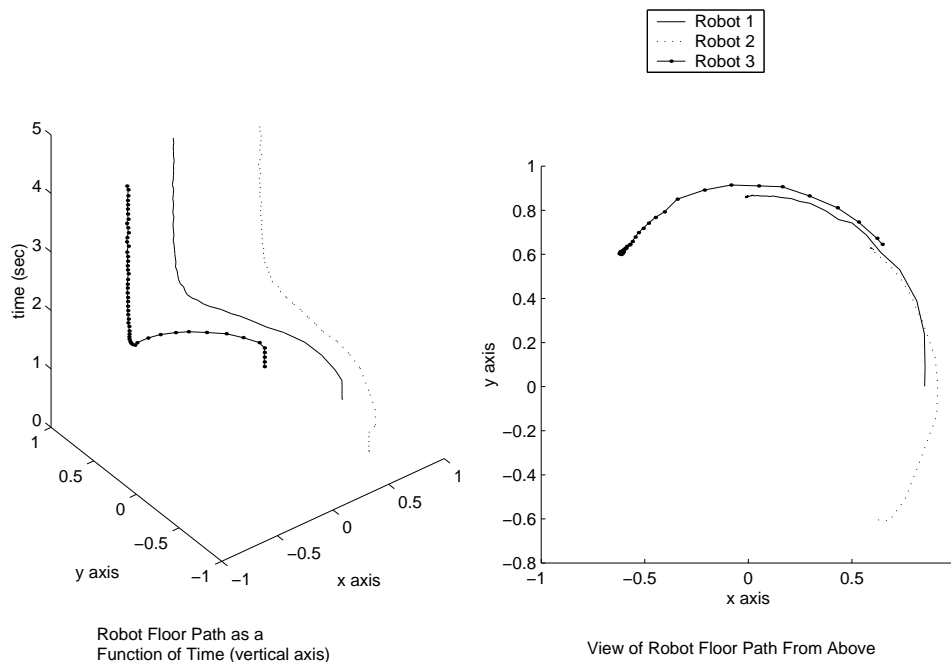


Fig. 7. Hardware Results: Floor Paths of Three Robot Formation.

tion can be describe by implementing combinations of these three EFMs in succession. Establishing the idea of EFMs simplifies the implementation of leader-following, virtual structure control and Behavior Based control.

By considering EFMs, appropriate coordinates can be chosen that allow us to arrive at greatly simplified system dynamics via feedback linearization. For a particular EFM this also allows us to decouple the motion of each robot into a component in the direction of the formation motion and the other component perpendicular to the direction of the formation motion. In a future paper, we will consider exploiting this “decoupling” aspect of the coordinate transformation to generate savings in inter-robot communication.

In this paper we used the behavioral based, coupled dynamics approach to implement EFMs. The advantage of the coupled dynamics approach is that it is decentralized and does not require relative velocity information among the robots. The main idea behind the algorithm is to include a global position term to ensure convergence and a relative position term to ensure formation keeping. We found that inter-robot damping can be adequately injected via an additional passivity-based control term. This allows the robots to perform their formation control maneuvers without relative velocity information. It is

also observed that actuator saturation can be taken directly into account with the modified coupled dynamics control presented in Theorem III.3.

Simulation and hardware results were included to illustrate the effectiveness of the coupled dynamics control.

ACKNOWLEDGMENT

We acknowledge partial funding for the first author from Jet Propulsion Laboratory, California Institute of Technology under contract #96-1245 and by a Rocky Mountain NASA Space Grant Consortium Fellowship. We also acknowledge partial funding for the second author by a BYU College of Engineering grant. We would like to thank Tim Gold and Chad Humberstone for their assistance with the robot testbed. We would also like to acknowledge useful discussions with Wynn Stirling, Mike Goodrich, Rick Frost and Kevin Smith.

REFERENCES

- [1] William C. Dickson, Robert H. Cannon, and Stephan M. Rock, "Symbolic dynamic modeling and analysis of object/robot-team systems with experiments," in *Proceedings of the IEEE Conference on Robotics and Automation*, Minneapolis, Minnesota, April 1996, pp. 1413–1420.
- [2] C. Ronald Kube and Hong Zhang, "The use of perceptual cues in multi-robot box-pushing," in *Proceedings of the IEEE International Conference on Robotics and Automation*, Minneapolis, Minnesota, April 1996, pp. 2085–2090.
- [3] Thierry Vidal, Malik Ghallab, and Rachid Alami, "Incremental mission allocation to a large team of robots," in *Proceedings of the IEEE International Conference on Robots and Automation*, Minneapolis Minnesota, April 1996, pp. 1620–1625.
- [4] Daisuke Kurabayashi, Jun Ota, Tamio Arai, and Eiichi Yoshida, "Cooperative sweeping by multiple mobile robots," in *Proceedings of the IEEE International Conference on Robotics and Automation*, Minneapolis, Minnesota, April 1996, pp. 1744–1749.
- [5] M.O. Anderson, M.D. Mckay, and B.S. Richardson, "Multirobot automated indoor floor characterization team," in *Proceedings of the IEEE Conference on Robotics and Automation*, Minneapolis, Minnesota, April 1996, pp. 1750–1753.
- [6] Hiroaki Yamaguchi, "Adaptive formation control for distributed autonomous mobile robot groups," in *Proceedings of the IEEE International Conference on Robotics and Automation*, Albuquerque, New Mexico, April 1997, pp. 2300–2305.
- [7] Randal W. Beard, Jonathan Lawton, and Fred Y. Hadaegh, "A coordination architecture for spacecraft formation control," *IEEE Control Systems Technology*, Submitted, Available at <http://www.ee.byu.edu/~beard/papers/cst99.ps>.

- [8] P. K. C. Wang, "Navigation strategies for multiple autonomous mobile robots moving in formation," *Journal of Robotic Systems*, vol. 8, no. 2, pp. 177–195, 1991.
- [9] P. K. C. Wang and F. Y. Hadaegh, "Coordination and control of multiple microspacecraft moving in formation," *The Journal of the Astronautical Sciences*, vol. 44, no. 3, pp. 315–355, 1996.
- [10] P.K.C. Wang, F.Y. Hadaegh, and K. Lau, "Synchronized formation rotation and attitude control of multiple free-flying spacecraft," *AIAA Journal of Guidance, Control and Dynamics*, vol. 22, no. 1, pp. 28–35, January 1999.
- [11] Fred Y. Hadaegh, Wei-Min Lu, and Paul K. C. Wang, "Adaptive control of formation flying spacecraft for interferometry," in *IFAC. IFAC*, 1998.
- [12] Thomas Sugar and Vijay Kumar, "Decentralized control of cooperating mobile manipulators," in *Proceedings of the IEEE International Conference on Robotics and Automation*, Leuven, Belgium, May 1998, pp. 2916–2921.
- [13] Jaydev P. Desai, Jim Ostrowski, and Vijay Kumar, "Controlling formations of multiple mobile robots," in *Proceedings of the IEEE International Conference on Robotics and Automation*, Leuven, Belgium, May 1998, pp. 2864–2869.
- [14] Hiroacki Yamaguchi and Joel W. Burdick, "Asymptotic stabilization of multiple nonholonomic mobile robots forming group formations," in *Proceedings of the IEEE International Conference on Robotics and Automation*, Leuven, Belgium, May 1998, pp. 3573–3580.
- [15] Colin R. McInnes, "Autonomous ring formation for a planar constellation of satellites," *Journal of Guidance, Control and Dynamics*, vol. 18, no. 5, pp. 1215–1217, 1995.
- [16] Mark R. Anderson and Andrew C. Robbins, "Formation flight as a cooperative game," in *Proceedings of the AIAA Guidance, Navigation and Control Conference*, Boston, MA, August 1998, American Institute of Aeronautics and Astronautics, pp. 244–251, AIAA-98-4124.
- [17] Tucker Balch and Ronald C. Arkin, "Behavior-based formation control for multirobot teams," *IEEE Transactions on Robotics and Automation*, vol. 14, no. 6, pp. 926–939, December 1998.
- [18] Xiaoping Yun, Gokhan Alptekin, and Okay Albayrak, "Line and circle formation of distributed physical mobile robots," *Journal of Robotic Systems*, vol. 14, no. 2, pp. 63–76, 1997.
- [19] Qin Chen and J. Y. S. Luh, "Coordination and control of a group of small mobile robots," in *Proceedings of the IEEE International Conference on Robotics and Automation*, 1994, pp. 2315–2320.
- [20] Kar-Han Tan and M. Anthony Lewis, "Virtual structures for high-precision cooperative mobile robot control," *Autonomous Robots*, vol. 4, no. 4, pp. 387–403, October 1997.
- [21] Randal W. Beard and Fred Y. Hadaegh, "Constellation templates: An approach to autonomous formation flying," in *World Automation Congress*, Anchorage, Alaska, May 1998, pp. 177.7–177.6, ISIAAC.
- [22] Randal Beard, "Architecture and algorithms for constellation control," Technical Report, Jet Propulsion Laboratory, California Institute of Technology, 4800 Oak Grove Dr., Pasadena, CA 91109, March 1998.
- [23] R. W. Brockett, "Asymptotic stability and feedback stabilization," in *Differential Geometric Control Theory*, R. S. Millman and H. J. Sussmann, Eds. 1983, pp. 181–191, Birkhäuser.
- [24] Alessandro Astolfi, "Exponential stabilization of a wheeled mobile robot via discontinuous control," *ASME, Journal of Dynamic Systems Measurement and Control*, March 1999.
- [25] C. Canudas de Wit and O.J. Sordalen, "Exponential stabilization of mobile robots with nonholonomic constraints," *IEEE Transactions On Automatic Control*, vol. 37, no. 11, pp. 1791–1797, November 1992.

- [26] Claude Samson, "Time-varying feedback stabilization of car-like wheeled mobile robots," *The International Journal of Robotics Research*, vol. 12, no. 1, pp. 55–64, February 1993.
- [27] J.-B. Pomet, B. Thuilot, G. Bastin, and G. Campion, "A hybrid strategy for the feedback stabilization of nonholonomic mobile robots," in *Proceedings of the IEEE International Conference on Robotics and Automation*, Nice, France, May 1992, pp. 129–134.
- [28] Claude Samson and K. Ait-Abderrahim, "Feedback control of a nonholonomic wheeled cart in cartesian space," in *Proceedings of the International Conference on Robotics and Automation*, Sacramento, California, April 1991, IEEE, pp. 1136–1139, Tracking Paper - as long as you don't stop.
- [29] Scharf, *Statistical Signal Processing: Detection, Estimation, and Time Series Analysis*, chapter 2, pp. 69–70, Addison-Wesley, 1991.
- [30] Romeo Ortega, Antonio Loria, Rafael Kelly, and Luarent Praly, "On passivity-based output feedback global stabilization of Euler-Lagrange systems," *International Journal Of Robust and Nonlinear Control*, vol. 5, pp. 313–323, 1995.
- [31] Fernando Lizarralde and John Wen, "Attitude control without angular velocity measurement: A passivity approach," *IEEE Transaction On Automatic Control*, vol. 41, no. 3, pp. 468–472, March 1996.
- [32] Panagiotis Tsiotras, "Further passivity results for the attitude control problem," *IEEE Transaction On Automatic Control*, vol. 43, no. 11, pp. 1597–1600, 1998.
- [33] Alexander Graham, *Kronecker Products and Matrix Calculus:with Applications*, Halsted Press, 1981, Properties of Kronecker Products.
- [34] William H. Beyer, Ed., *CRC Standard Mathematical Tables*, CRC Press, Inc, Boca Raton, Florida, 27 edition, 1984.